

Lawrence Berkeley National Laboratory

Lawrence Berkeley National Laboratory

Title

The low energy spectrum of TeO₂ bolometers: results and perspectives for the CUORE-0 and CUORE experiments

Permalink

<https://escholarship.org/uc/item/0v875408>

Author

Alessandria, F.

Publication Date

2013-01-29

The low energy spectrum of TeO₂ bolometers: results and perspectives for the CUORE-0 and CUORE experiments

F. Alessandria,¹ R. Ardito,² D. R. Artusa,^{3,4} F. T. Avignone III,³ O. Azzolini,⁵ M. Balata,⁴ T. I. Banks,^{6,7,4} G. Bari,⁸ J. Beeman,⁹ F. Bellini,^{10,11} A. Bersani,¹² M. Biassoni,^{13,14} T. Bloxham,⁷ C. Brofferio,^{13,14} C. Bucci,⁴ X. Z. Cai,¹⁵ L. Canonica,⁴ S. Capelli,^{13,14} L. Carbone,¹⁴ L. Cardani,^{10,11} M. Carrettoni,^{13,14} N. Casali,⁴ N. Chott,³ M. Clemenza,^{13,14} C. Cosmelli,^{10,11} O. Cremonesi,¹⁴ R. J. Creswick,³ I. Dafinei,¹¹ A. Dally,¹⁶ V. Datskov,¹⁴ A. De Biasi,⁵ M. P. Decowski,^{7,6,*} M. M. Deninno,⁸ S. Di Domizio,^{17,12} M. L. di Vacri,⁴ L. Ejzak,¹⁶ R. Faccini,^{10,11} D. Q. Fang,¹⁵ H. A. Farach,³ E. Ferri,^{13,14} F. Ferroni,^{10,11} E. Fiorini,^{14,13} M. A. Franceschi,¹⁸ S. J. Freedman,^{7,6} B. K. Fujikawa,⁷ A. Giachero,¹⁴ L. Gironi,^{13,14} A. Giuliani,¹⁹ J. Goett,⁴ P. Gorla,²⁰ C. Gotti,^{13,14} E. Guardincerri,^{4,7,†} T. D. Gutierrez,²¹ E. E. Haller,^{9,22} K. Han,⁷ K. M. Heeger,¹⁶ H. Z. Huang,²³ R. Kadel,²⁴ K. Kazkaz,²⁵ G. Keppel,⁵ L. Kogler,^{7,6,‡} Yu. G. Kolomensky,^{6,24} D. Lenz,¹⁶ Y. L. Li,¹⁵ C. Ligi,¹⁸ X. Liu,²³ Y. G. Ma,¹⁵ C. Maiano,^{13,14} M. Maino,^{13,14} M. Martinez,²⁶ R. H. Maruyama,¹⁶ N. Moggi,⁸ S. Morganti,¹¹ T. Napolitano,¹⁸ S. Newman,^{3,4} S. Nisi,⁴ C. Nones,²⁷ E. B. Norman,^{25,28} A. Nucciotti,^{13,14} F. Orio,¹¹ D. Orlandi,⁴ J. L. Ouellet,^{6,7} M. Pallavicini,^{17,12} V. Palmieri,⁵ L. Pattavina,¹⁴ M. Pavan,^{13,14} M. Pedretti,²⁵ G. Pessina,¹⁴ S. Pirro,¹⁴ E. Previtali,¹⁴ V. Rampazzo,⁵ F. Rimondi,^{29,8,§} C. Rosenfeld,³ C. Rusconi,¹⁴ S. Sangiorgio,²⁵ N. D. Scielzo,²⁵ M. Sisti,^{13,14} A. R. Smith,³⁰ F. Stivanello,⁵ L. Taffarello,³¹ M. Tenconi,¹⁹ W. D. Tian,¹⁵ C. Tomei,¹¹ S. Trentalange,²³ G. Ventura,^{32,33} M. Vignati,¹¹ B. S. Wang,^{25,28} H. W. Wang,¹⁵ C. A. Whitten Jr.,^{23,§} T. Wise,¹⁶ A. Woodcraft,³⁴ L. Zanotti,^{13,14} C. Zarra,⁴ B. X. Zhu,²³ and S. Zucchelli^{29,8}

¹INFN - Sezione di Milano, Milano I-20133 - Italy

²Dipartimento di Ingegneria Strutturale, Politecnico di Milano, Milano I-20133 - Italy

³Department of Physics and Astronomy, University of South Carolina, Columbia, SC 29208 - USA

⁴INFN - Laboratori Nazionali del Gran Sasso, Assergi (L'Aquila) I-67010 - Italy

⁵INFN - Laboratori Nazionali di Legnaro, Legnaro (Padova) I-35020 - Italy

⁶Department of Physics, University of California, Berkeley, CA 94720 - USA

⁷Nuclear Science Division, Lawrence Berkeley National Laboratory, Berkeley, CA 94720 - USA

⁸INFN - Sezione di Bologna, Bologna I-40127 - Italy

⁹Materials Science Division, Lawrence Berkeley National Laboratory, Berkeley, CA 94720 - USA

¹⁰Dipartimento di Fisica, Sapienza Università di Roma, Roma I-00185 - Italy

¹¹INFN - Sezione di Roma, Roma I-00185 - Italy

¹²INFN - Sezione di Genova, Genova I-16146 - Italy

¹³Dipartimento di Fisica, Università di Milano-Bicocca, Milano I-20126 - Italy

¹⁴INFN - Sezione di Milano Bicocca, Milano I-20126 - Italy

¹⁵Shanghai Institute of Applied Physics (Chinese Academy of Sciences), Shanghai 201800 - China

¹⁶Department of Physics, University of Wisconsin, Madison, WI 53706 - USA

¹⁷Dipartimento di Fisica, Università di Genova, Genova I-16146 - Italy

¹⁸INFN - Laboratori Nazionali di Frascati, Frascati (Roma) I-00044 - Italy

¹⁹Centre de Spectrométrie Nucléaire et de Spectrométrie de Masse, 91405 Orsay Campus - France

²⁰INFN - Sezione di Roma Tor Vergata, Roma I-00133 - Italy

²¹Physics Department, California Polytechnic State University, San Luis Obispo, CA 93407 - USA

²²Department of Materials Science and Engineering,

University of California, Berkeley, CA 94720 - USA

²³Department of Physics and Astronomy, University of California, Los Angeles, CA 90095 - USA

²⁴Physics Division, Lawrence Berkeley National Laboratory, Berkeley, CA 94720 - USA

²⁵Lawrence Livermore National Laboratory, Livermore, CA 94550 - USA

²⁶Laboratorio de Fisica Nuclear y Astroparticulas,

Universidad de Zaragoza, Zaragoza 50009 - Spain

²⁷Service de Physique des Particules, CEA / Saclay, 91191 Gif-sur-Yvette - France

²⁸Department of Nuclear Engineering, University of California, Berkeley, CA 94720 - USA

²⁹Dipartimento di Fisica, Università di Bologna, Bologna I-40127 - Italy

³⁰EH&S Division, Lawrence Berkeley National Laboratory, Berkeley, CA 94720 - USA

³¹INFN - Sezione di Padova, Padova I-35131 - Italy

³²Dipartimento di Fisica, Università di Firenze, Firenze I-50125 - Italy

³³INFN - Sezione di Firenze, Firenze I-50125 - Italy

³⁴SUPA, Institute for Astronomy, University of Edinburgh, Blackford Hill, Edinburgh EH9 3HJ - UK

We collected 19.4 days of data from four 750 g TeO₂ bolometers, and in three of them we were able to set the energy threshold around 3 keV using a new analysis technique. We found a background rate ranging from 25 cpd/keV/kg at 3 keV to 2 cpd/keV/kg at 25 keV, and a peak at 4.7 keV. The origin of this peak is presently unknown, but its presence is confirmed by a reanalysis of 62.7 kg-days

of data from the finished CUORICINO experiment. Finally, we report the expected sensitivities of the CUORE-0 (52 bolometers) and CUORE (988 bolometers) experiments to a WIMP annual modulation signal.

PACS numbers: 07.57.Kp, 29.85.Ca, 95.35.+d

Keywords: Bolometers, Nuclear Physics, Dark Matter

DISCLAIMER: This document was prepared as an account of work sponsored by the United States Government. While this document is believed to contain correct information, neither the United States Government nor any agency thereof, nor the Regents of the University of California, nor any of their employees, makes any warranty, express or implied, or assumes any legal responsibility for the accuracy, completeness, or usefulness of any information, apparatus, product, or process disclosed, or represents that its use would not infringe privately owned rights. Reference herein to any specific commercial product, process, or service by its trade name, trademark, manufacturer, or otherwise, does not necessarily constitute or imply its endorsement, recommendation, or favoring by the United States Government or any agency thereof, or the Regents of the University of California. The views and opinions of authors expressed herein do not necessarily state or reflect those of the United States Government or any agency thereof or the Regents of the University of California.

I. INTRODUCTION

Tellurium dioxide bolometers are excellent detectors to search for rare processes. Operated at a temperature of about 10 mK, these detectors feature an energy resolution of a few keV over an energy range extending from a few keV up to several MeV. This, together with the low level of radioactive background achievable and the low cost, makes them ideal detectors for CUORE, an experiment that will search for neutrinoless double beta decay ($0\nu\text{DBD}$) of ^{130}Te [1, 2].

CUORE will consist of 988 TeO_2 bolometers of 750 g each and is expected to reach a background level at the ^{130}Te Q-value (around 2528 keV [3–5]) of the order of 0.01 counts/keV/kg/y, thus allowing a sensitivity to $0\nu\text{DBD}$ down to the inverted hierarchy of neutrino masses. CUORE is currently being installed at the Laboratori Nazionali del Gran Sasso (LNGS) in Italy and is

scheduled to start taking data in 2014. The experimental design was validated by CUORICINO, an array of 62 TeO_2 bolometers (for total mass of 40.7 kg) which took data at LNGS from 2003 to 2008 and put stringent limits on the $0\nu\text{DBD}$ half-life [6, 7]. To test the new assembly line and the materials chosen for CUORE, an array of 52 TeO_2 bolometers, named CUORE-0, has been recently built. It is expected to have a smaller background than CUORICINO and will start taking data in Fall 2012.

Given the high mass, the good energy resolution, and the low background, the CUORE-0 and CUORE experiments can search for rare processes other than $0\nu\text{DBD}$. In particular, provided the energy threshold of few keV, they could look also for Dark Matter interactions. Such searches were not performed in CUORICINO because the energy threshold was too high, of the order of tens of keV. A new software trigger was developed to lower the energy threshold [8]. The trigger is based on the matched filter algorithm [9, 10] and also provides a pulse shape parameter to suppress false signals generated by detector vibrations and electronics noise.

In this paper we show the energy spectrum of four TeO_2 bolometers originally operated at LNGS in order to test the performances of CUORE crystals [11]. In three of them we were able to set the energy threshold around 3 keV, while in the fourth to 10 keV because of the high detector noise. The energy spectrum of the three bolometers exhibits a peak at 4.7 keV whose origin is presently unknown. The peak has a constant rate in time, and its presence is confirmed by a reanalysis of the data from the last two months of operation of CUORICINO. Given the observed counting rate, we also evaluate the sensitivity of CUORE-0 and CUORE to an annual modulation signal induced by WIMP Dark Matter candidates.

II. EXPERIMENTAL SETUP

A CUORE bolometer is composed of two main parts: a TeO_2 crystal and a neutron transmutation doped Germanium (NTD-Ge) thermistor [12, 13]. The crystal, a 750 g cube of side length 5 cm, is held by PTFE supports in copper frames. The frames are connected to the mixing chamber of a dilution refrigerator, which keeps the bolometers at a temperature of about 10 mK. The thermistor is glued to the crystal and acts as thermometer. The temperature increase due to an energy deposition in the crystal is measured by the increase in the resistance of the thermistor [14–16]. The thermistor is biased by a constant current and a change in the voltage across it constitutes the signal [17]. In the setup

* Presently at: Nikhef, 1098 XG Amsterdam - The Netherlands

† Presently at: Los Alamos National Laboratory, Los Alamos, NM 87545 - USA

‡ Presently at: Sandia National Laboratories, Livermore, CA 94551 - USA

§ Deceased

presented in this paper, called CUORE Crystal Validation Run 2 (CCVR2), each crystal was provided with two thermistors for redundancy. Two Joule heaters were also glued on two crystals and used to inject heat pulses with controlled amounts of energy to monitor the detector gain and detector efficiencies [18–20]. The bolometers were operated in the cryogenic R&D facility of CUORE whose details can be found in Refs. [21–23].

Data were collected over 23 days with small interruptions for calibrations and cryostat maintenance. The effective live time amounted to 19.4 days. On each of the four bolometers, labeled B1, B2, B3 and B4, we selected the thermistor in which the trigger reached the lowest energy threshold.

III. DETECTOR PERFORMANCE

The energy resolution was evaluated both at the baseline level and on the lowest energy peak in the spectrum. Randomly triggered events, not containing pulses, were used to evaluate the fluctuation of the baseline after the application of the matched filter. A Gaussian fit was performed on the 30.5 keV Sb line, which is due to EC decays of Te isotopes produced by cosmogenic activation during production and air-shipment of the crystals outside the underground laboratory. As one can see from Tab. I, baseline and 30.5 keV resolutions are quite close, since at these energies the resolution of bolometers is expected to be dominated by the noise. The bolometers feature excellent energy resolution, with B2, B3, and B4 below 1 keV FWHM, and B1 at 3.3 keV FWHM.

The detection efficiencies were measured via an energy scan performed at the end of the run by using the Joule heaters to provide sequences of pulses from 1 to 50 keV. However, heater events and actual particle events have slightly different pulse shapes which could result in slightly different energies and detection efficiencies. The trigger efficiency and any differences that may result from the difference between the heater pulses and particle events were investigated by Monte Carlo simulations.

Heater pulses between 1–50 keV and particle pulses in the same energy range were simulated separately using the tools described in Ref. [24]. Only B2 and B3 were simulated for heater pulses while all the four bolometers were considered for the particle pulses simulation. Both Monte Carlo runs included simulated detector noise and the background from particle pulses, randomly generated to match the event rate and the entire measured energy spectrum from threshold up to 5.4 MeV, i.e. the energy of ^{210}Po decays in the crystal. We processed the output of the simulation in the same way as the heater scan measurement. The estimated efficiencies on B2 are shown in Fig. 1, where the good agreement between Monte Carlo and data is evident.

The similarities in the energy dependence demonstrate that the trigger acts in the same way on particle and

heater pulses. This feature is visible also on B3, the other bolometer with a heater. We estimate the detection efficiencies on the two bolometers without heater (B1 and B4) using the Monte Carlo. For each bolometer, we evaluate the energy threshold for the data analysis as the energy at which the plateau is reached. The detection efficiency ϵ_D was computed as the weighted average of each point in the plateau. The energy threshold, the heater-measured, and particle-simulated detection efficiencies of each bolometer are reported in Tab. I.

Table I. Baseline resolution (ΔE_{base}), resolution at 30.5 keV ($\Delta E_{30 \text{ keV}}$), software energy threshold (θ_E) and detection efficiencies measured with the Joule heater ($\epsilon_D^{\text{heater}}$) and estimated from the Monte Carlo simulation of the four bolometers (ϵ_D^{MC}).

Bolo	ΔE_{base} [keV]	$\Delta E_{30 \text{ keV}}$ [keV FWHM]	θ_E [keV]	$\epsilon_D^{\text{heater}}$	ϵ_D^{MC}
B1	3.3	3.3 ± 0.7	10.0	n/a	0.878 ± 0.002
B2	0.66	0.53 ± 0.08	3.0	0.910 ± 0.005	0.913 ± 0.001
B3	0.76	0.83 ± 0.09	2.5	0.828 ± 0.007	0.825 ± 0.001
B4	0.82	0.59 ± 0.12	2.5	n/a	0.828 ± 0.002

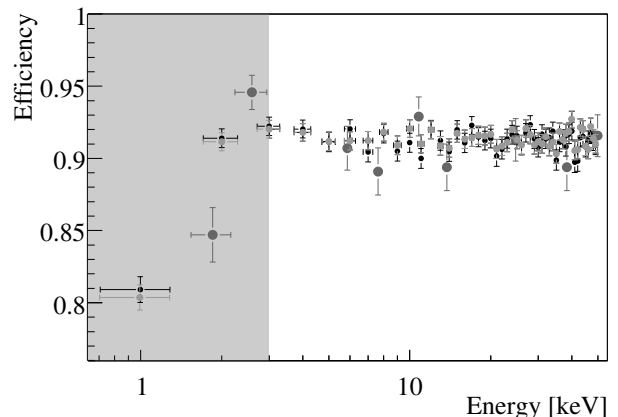


Figure 1. Detection efficiency on B2: particle Monte Carlo in black circles, heater Monte Carlo in gray circles, heater scan data in big circles. The shadowed band represents the region below the energy threshold chosen for the data analysis.

IV. ENERGY CALIBRATION

The energy calibration was performed by inserting two wires of thoriated tungsten in proximity of the detector, between the cryostat and the lead shields placed externally. The main γ lines of ^{232}Th , ranging from 511 to 2615 keV, and the lines generated by metastable Te isotopes in the crystals, ranging from 30 to 150 keV, were used for the determination of the calibration function (a

third order polynomial). The residual difference with respect to the nominal energy of the peaks in the low energy spectrum is shown in Fig. 2.

The calibration accuracy at energies lower than 30 keV was verified by using events from ^{121}Te and ^{40}K contaminations in the crystals. These isotopes may decay via EC to ^{121}Sb and ^{40}Ar , respectively, with the emission of a γ -ray from the daughter nucleus de-excitation (507.6 keV or 573.1 keV from ^{121}Te and 1461 keV from ^{40}K) and the de-excitation of the atomic shell L_1 and K ($E_{L_1} = 4.6983$ keV or $E_K = 30.4912$ keV from ^{121}Te and $E_K = 3.2060$ keV from ^{40}K). The atomic de-excitation process is fully contained in the crystal while, in some cases, the γ can escape and hit another crystal, thus producing a double hit event. We selected double hit events requiring that in one of the two crystals there is an energy release corresponding to the γ -rays from ^{121}Te or ^{40}K , and then we looked at the energy of the other crystal in the range 0–40 keV (Fig. 3). Two events from ^{40}K were found (3.04 and 3.18 keV) three from the L_1 (4.48, 4.67 and 4.74 keV), and ten from the K de-excitation after the ^{121}Te decay (30.53 ± 0.04 keV). Since all the events are compatible with their expected energy, the accuracy of the low-energy calibration is confirmed. We also noted that the K/L capture ratio for ^{121}Te is compatible within two standard deviations with the expected value of 7 [25].

As a further check of the goodness of our calibration, we placed a ^{55}Fe source next to a bolometer. The X-rays produced, with nominal energy between 5.888 and 6.490 keV, resulted in detected energies that were shifted, on average, by only 48 ± 16 eV from their nominal values.

V. EVENT SELECTION

We selected signal events using the shape indicator variable (SI) described in Ref. [8]. This variable is based on the χ^2 of the fit of the waveforms with the expected

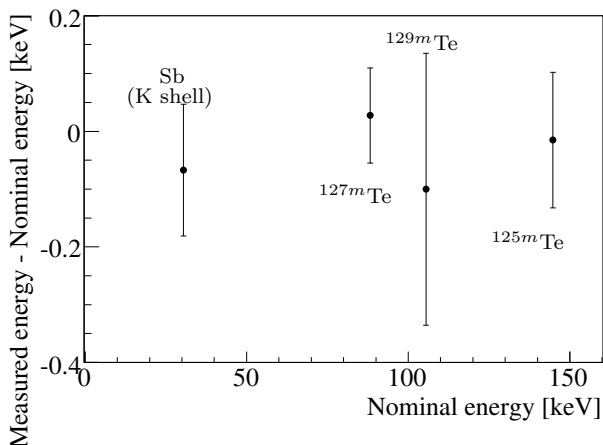


Figure 2. Residuals of the calibration function of B2 on metastable Te lines.

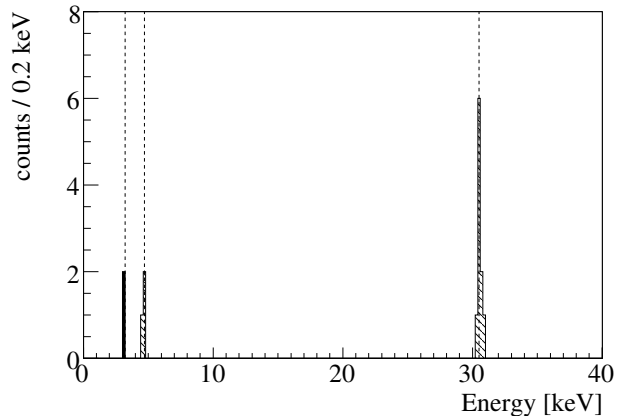


Figure 3. Summed energy spectrum from B2, B3 and B4 in time coincidence with an energy deposition on another bolometer (including B1) compatible with the γ lines from ^{40}K (solid) or ^{121}Te decays (hashed). The dashed lines represent the nominal values of the de-excitation energies. No event is observed away from these lines.

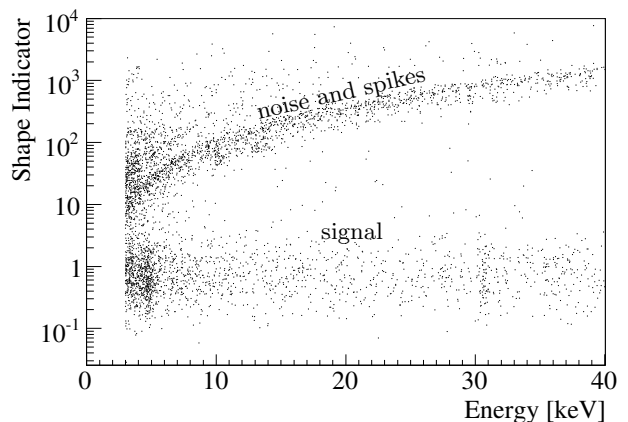


Figure 4. Pulse shape indicator (SI) distribution on B2. The band at low SI is populated by signal events. At higher values there are triggered mechanic vibrations, electronic spikes and pileups. The optimal cut for this bolometer was found to be $\text{SI} < 2.2$.

shape of the signal. The distribution of SI versus energy for B2 is shown in Fig. 4. The signal region is easily identified, and a considerable part of the pulses generated by thermal and electronic noise can be removed with a cut on this variable.

We evaluated the optimal value of the cut on SI using the Sb K line at 30.5 keV. We performed a series of extended unbinned maximum-likelihood fits, selecting the events below a fixed SI value. For each SI cut, the spectra of cut accepted events and cut rejected events were simultaneously fitted with a Gaussian, representative of the signal, plus a first-order polynomial function, representative of the background. Signal (ϵ_S) and back-

ground (ϵ_B) efficiencies after the cut were evaluated directly in the fit. For each bolometer we selected the cut which maximized the statistical significance, defined as $\epsilon_S/\sqrt{\epsilon_B}$, corresponding in this case to $\epsilon_S = 1$.

VI. MEASURED SPECTRA

The energy spectra of the four detectors show several γ and α peaks that are clearly identified as due to U, Th and K contaminations (of the crystals themselves and of the experimental setup) and few low energy peaks identified as being due to Te metastable isotopes. The region between threshold and 40 keV is shown in Fig. 5. In the three bolometers with the lowest threshold, a peak appears at about 4.7 keV, the energy of the L_1 atomic shell of Sb. This in principle indicates that the line could be ascribed to the EC decay of a Te isotope, however none of the known or predicted isotope decays can explain our observation:

- The ^{121m}Te and its daughter ^{121}Te decay via EC with half-lives of 154 and 17 days, respectively. However the intensity of the observed peak is higher than the K line of Sb at 30.5 keV. This is in contradiction with the measured value of the K/ L_1 capture ratio for these isotopes which is greater than one.
- The other EC decaying metastable Te isotopes (and their daughters) have half-lives smaller than 4.7 days. As it will be demonstrated later, the observed peak rate is constant over 20 days.
- ^{123}Te is a naturally occurring isotope of Tellurium (abundance $0.908 \pm 0.002\%$ [26]) which may decay via EC to ^{123}Sb with a Q-value of 52.2 ± 1.5 keV. Since the transition is 2nd-forbidden unique, it has been estimated that very little K capture actually occurs and that the majority of EC decays take

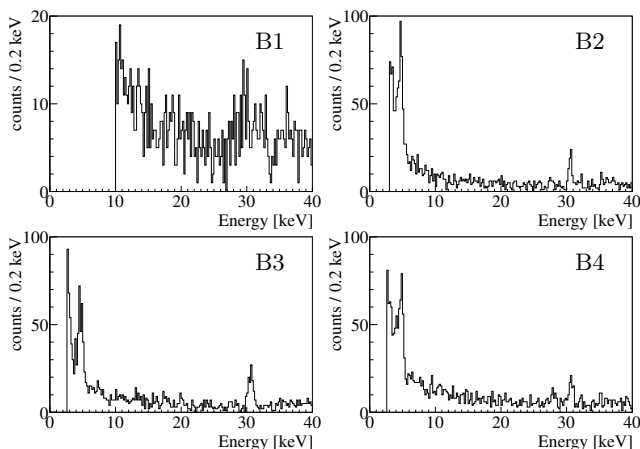


Figure 5. Low energy spectra of the four bolometers. Full statistics (19.4 days) with pulse shape cut applied.

Table II. Best fit results for the 4.7 keV line and estimated peaking background from ^{121}Te . The error on the energy includes the systematic due to the calibration.

Bolometer	Energy [keV]	FWHM [keV]	N_{sig} [counts]	N_{121} [counts]
B2	4.75 ± 0.28	0.57 ± 0.11	191^{+41}_{-31}	6.1 ± 1.3
B3	4.66 ± 0.28	0.87 ± 0.10	255^{+51}_{-35}	13.5 ± 1.6
B4	4.76 ± 0.38	0.75 ± 0.12	205^{+45}_{-34}	7.5 ± 1.4

place from the L_3 shell. Several searches for Sb K lines from EC of ^{123}Te have been performed. Positive evidence, $T_{1/2} = (1.24 \pm 0.10) \cdot 10^{13}$ y, was claimed by Watt and Glover [27] but subsequently ruled out [28, 29]. In this paper, we show for the first time an energy spectrum down to the L energy region. The line we observe however cannot be attributed to ^{123}Te , since, as described in the next section, the energy is compatible with the L_1 shell (4.6983 keV) and not with the L_3 one (4.1322 keV).

VII. ANALYSIS OF THE 4.7 KEV PEAK

In the following we report the analysis of the peak in the energy distribution of single bolometers, to provide all the possible details and to stimulate a discussion within the scientific community that will hopefully lead to its identification. To determine the intensity, the peaking background due to the EC decay of ^{121m}Te – ^{121}Te was removed. The γ -rays produced by these isotopes can escape without hitting another crystal, such that only the K or the L de-excitations are measured. The number of pure L events from ^{121}Te and ^{121m}Te (N_{121}) were estimated using a Monte Carlo simulation based on GEANT4 [30], normalizing the single hit spectra to the measured rate of the most intense ^{121m}Te peak (294.0 keV).

To estimate the intensity and the energy of the line from the data, we performed a separate extended unbinned maximum-likelihood fit for each bolometer, using a likelihood function constituted by a Gaussian plus two exponential functions to reproduce the background. We set the pulse shape cuts at the estimated optimal values. The selection efficiencies were recomputed on the peak at 4.7 keV, since the events in this peak are more plentiful than in the Sb K peak at 30.5 keV. The obtained number of events N_e was then corrected taking into account the detection and cut efficiencies and the expected background N_{121} , according to the equation $N_{sig} = (N_e - N_{121})/(\epsilon_D \epsilon_S)$. Best fits are shown in Fig. 6. In Tab. II we report the summary of the peak parameters of each bolometer, also including the estimated peaking background N_{121} .

We combined the profile negative log-likelihoods of N_e and N_{121} of the three bolometers (Fig. 6) to compute

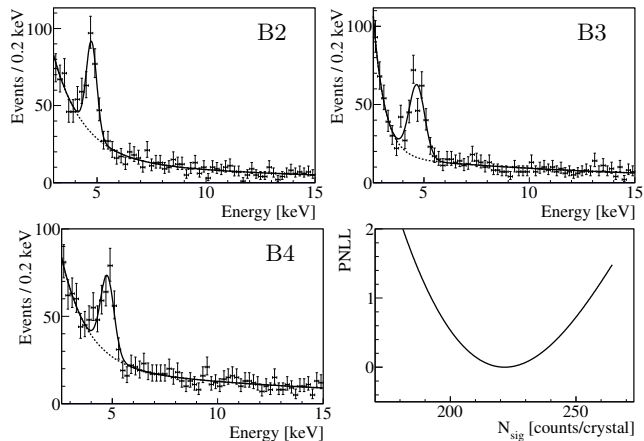


Figure 6. Best fits at the 4.7 keV line on the three bolometers with low threshold. On the bottom right, the combined profile negative log-likelihood projected over the number of signal events.

the average rate. The estimated value of the number of signal events is 223 ± 22 counts/crystal, from which we evaluated the line intensity in TeO_2 to be $I = 15.3 \pm 1.5$ counts/day/kg. The energy averaged over the three bolometers is 4.72 ± 0.18 keV.

Figure 7 shows the peak rate along the duration of the data-taking, which is in a very good agreement with a constant distribution, indicating that this signal is not due to a short-living radioactive contamination. It also indicates that any variation of the detection efficiency with time is negligible compared to the statistical error.

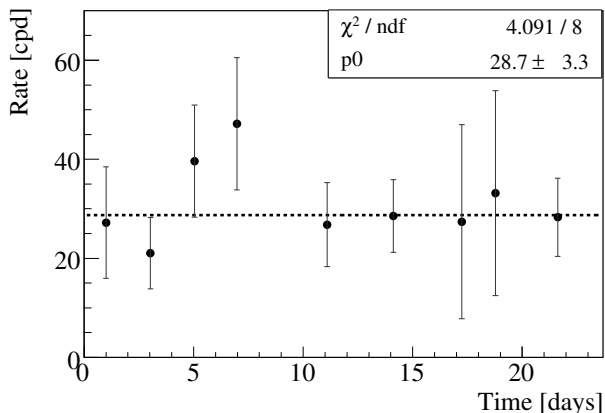


Figure 7. Rate of the 4.7 keV peak versus solar time in all three CCVR2 bolometers summed together. No variation is appreciable.

To check the stability of the line over a longer period of time, we checked its presence in the CUORICINO data. During the last two months of operation of CUORICINO, the data-acquisition system being developed for CUORE (the same used for CCVR2), was run in parallel with the old system, saving to disk the continuous stream

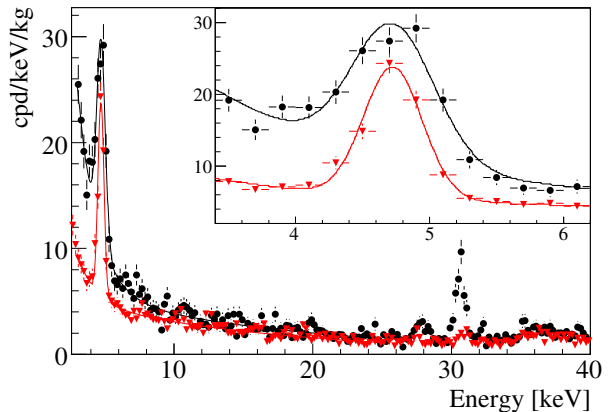


Figure 8. Comparison of CCVR2 (black circles) and CUORICINO (red triangles) data, with a zoom on the 4.7 keV. Unlike in CCVR2, CUORICINO data are not corrected for the efficiencies and the calibration at low energies is not optimized.

of data. The live-time of continuous data amounts to 47.5 days. We ran the new trigger on these data but we were able to reach a threshold below 4 keV only on 4 bolometers, because of the high vibrational noise transmitted by the holder to the crystals (CCVR, CUORE-0 and CUORE holders have been explicitly redesigned to lower the transmitted noise). These 4 bolometers had smaller size ($3 \times 3 \times 6$ cm³, 330 g) than other CUORICINO and CUORE bolometers, and featured higher signal to noise ratio.

The sum energy spectrum of the four bolometers is overlaid to the sum energy spectrum of the CCVR2 bolometers in Fig. 8. In CUORICINO the heater energy scan was not performed, therefore the spectrum shown is not corrected for the detection efficiencies. As it can be seen from the figure, the peak is very well visible, with a fitted energy resolution of 0.52 ± 0.04 keV FWHM. The intensity and the average energy are found to be similar to the CCVR2 ones, being $(10.0 \pm 0.6)/\epsilon$ counts/day/kg and 4.73 ± 0.01 keV, respectively. We also note that the 30.5 keV peak disappeared, because the $^{121m-121}\text{Te}$ isotopes decayed away during the 5 years of underground data taking. For this reason, the calibration is not as accurate at low energies. However, the error is expected to be less than 0.5 keV.

VIII. SENSITIVITY TO WIMPS

It has to be remarked that TeO_2 bolometers, unlike other bolometric detectors for Dark Matter, do not discriminate the nuclear recoils induced by WIMPs from the radioactive β/γ background. Nevertheless, the high mass and low background achievable with these detectors make it possible to search for an annual modulation of the counting rate.

Compared to CUORICINO, the CCVR2 rate has the same behavior at energies greater than 10 keV, but is considerably higher at lower energies (Fig. 8). We are unable to explain this difference at present, however we expect that the CUORE-0 and CUORE low energy background will not be higher than the CCVR2 one. All the materials used in detector construction, in fact, will be the same as those employed for CCVR2. Moreover, in the case of CUORE-0, the bolometers will be operated in the same cryostat of CUORICINO, which has lower radioactive contaminations compared to the one used to operate CCVR2. To be conservative, we estimate the CUORE-0 and CUORE sensitivity to WIMPs assuming the background rate of these experiments to be equal to the one measured on CCVR2. We assume that the noise will be under control and that all bolometers will achieve a 3 keV threshold. We focus on the energy region between threshold and 25 keV, featuring an observed background counting rate ranging from about 25 cpd/keV/kg to 2 cpd/keV/kg.

We perform toy Monte Carlo simulations generating background events from the CCVR2 fit function shown in Fig. 8, and WIMP events from the predicted distribution described in Ref. [31], using the following WIMP parameters: density $\rho_W = 0.3 \text{ GeV/cm}^3$, average velocity $v_0 = 220 \text{ km/s}$ and escape velocity from the Galaxy $v_{esc} = 600 \text{ km/s}$. The quenching factor (QF) of the interactions in TeO_2 is set to 1 [32]. We include the dependence of the WIMP interaction rate on the time in the year, and estimated the background+signal asymmetry subtracting the 3-month integrated spectrum across December the 2nd from the 3-month integrated spectrum across June the 2nd. The resulting differential spectrum is fitted with the expected shape induced by the modulation, H_1 (examples are given in Fig. 9), and with a flat line at zero counts, H_0 . The cross section in the toy simulation is lowered as long as, in a set of experiments, the fit probability of the H_1 hypothesis is greater than the H_0 one at least 90% of the times.

This procedure defines the cross section that could be sensed for a fixed WIMP mass. The 90% CL upper limit sensitivity to the cross-section as a function of the WIMP mass is reported in Fig. 10 for 3-years of CUORE-0 data-taking and 5-years of CUORE. The comparison with other experiments shows that CUORE-0 could test the indication of a $\sim 10 \text{ GeV}$ WIMP from the DAMA (no-channeling), CoGeNT and CRESST experiments, while CUORE could completely test the DAMA results, under the hypothesis that Dark Matter is made of WIMPs. We reiterate that because the quenching factor for nuclear recoils compared to electron recoils in TeO_2 bolometers is 1, the 2-6 keV energy region of DAMA corresponds to 7-20 keV assuming scattering on Na (QF=0.3) or 22-67 keV assuming scattering on I (QF=0.9). Therefore, in TeO_2 bolometers it will be possible to look at lower energies and to study with larger detail the shape of the modulation spectrum, thus providing new information to this complicated search.

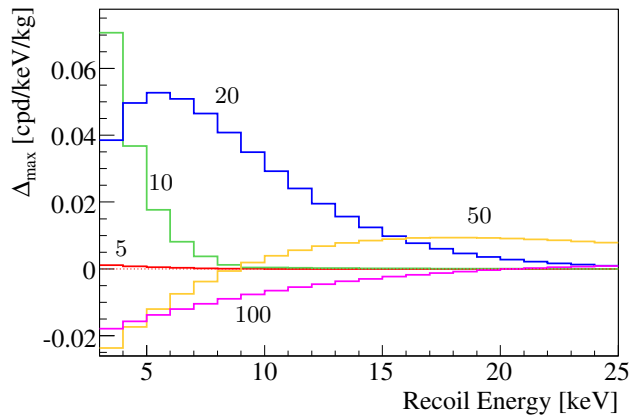


Figure 9. WIMP signal: difference between the 3-month integrated spectra across December the 2nd and June the 2nd, for a WIMP cross section of 10^{-41} cm^2 and masses between 5 and 100 GeV.

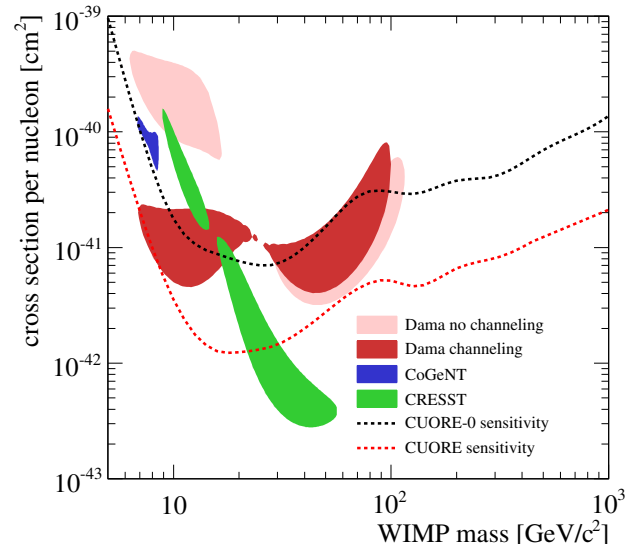


Figure 10. 90% sensitivity to WIMPs of CUORE-0 and CUORE assuming a 3 keV threshold for all detectors and the same background level of the CCVR2 detectors. Evidences of DAMA- 3σ [33], CoGeNT-90% [34] and CRESST- 2σ [35] are reported for comparison.

ACKNOWLEDGMENTS

The CUORE Collaboration thanks the Directors and Staff of the Laboratori Nazionali del Gran Sasso and the technical staffs of our Laboratories. This work was supported by the Istituto Nazionale di Fisica Nucleare (INFN); the Director, Office of Science, of the U.S. Department of Energy under Contract Nos. DE-AC02-05CH11231 and DE-AC52-07NA27344; the DOE

Office of Nuclear Physics under Contract Nos. DE-FG02-08ER41551 and DEFG03-00ER41138; the National Science Foundation under Grant Nos. NSF-PHY-0605119, NSF-PHY-0500337, NSF-PHY-0855314, and NSF-PHY-0902171; the Alfred P. Sloan Foundation; and the University of Wisconsin Foundation.

-
- [1] C. Arnaboldi *et al.*, *Astropart.Phys.*, **20**, 91 (2003), arXiv:hep-ex/0302021 [hep-ex].
- [2] C. Arnaboldi *et al.*, *Nucl. Instrum. Meth. A.*, **518**, 775 (2004), hep-ex/0212053v1.
- [3] M. Redshaw, B. J. Mount, E. G. Myers, and F. T. Avignone, *Phys. Rev. Lett.*, **102**, 212502 (2009).
- [4] N. D. Scielzo *et al.*, *Physical Review C*, **80**, 025501 (2009).
- [5] S. Rahaman, V. Elomaa, T. Eronen, J. Hakala, A. Jokinen, *et al.*, *Phys.Lett.*, **B703**, 412 (2011).
- [6] E. Andreotti *et al.*, *Astropart.Phys.*, **34**, 822 (2011), arXiv:1012.3266 [nucl-ex].
- [7] E. Andreotti *et al.*, *Phys.Rev.*, **C85**, 045503 (2012), arXiv:1108.4313 [nucl-ex].
- [8] S. Di Domizio, F. Orio, and M. Vignati, *JINST*, **6**, P02007 (2011), arXiv:1012.1263 [astro-ph.IM].
- [9] E. Gatti and P. F. Manfredi, *Riv. Nuovo Cimento*, **9**, 1 (1986).
- [10] V. Radeka and N. Karlovac, *Nucl. Instrum. Methods*, **52**, 86 (1967).
- [11] F. Alessandria, E. Andreotti, R. Ardito, C. Arnaboldi, I. Avignone, F.T., *et al.*, *Astropart.Phys.*, **35**, 839 (2012), arXiv:1108.4757 [nucl-ex].
- [12] N. Wang *et al.*, *Phys. Rev. B*, **41**, 3761 (1990).
- [13] K. M. Itoh *et al.*, *Appl. Phys. Lett.*, **64**, 2121 (1994).
- [14] N. F. Mott, *Phil. Mag.*, **19**, 835 (1969).
- [15] A. Efros and B. Shklovskii, "Electronic properties of doped semiconductors," (Springer-Verlag, Berlin, 1984) p. 202.
- [16] K. M. Itoh *et al.*, *Phys. Rev. Lett.*, **77**, 4058 (1996).
- [17] C. Arnaboldi *et al.*, *IEEE Trans. Nucl. Sci.*, **49**, 2440 (2002).
- [18] A. Alessandrello *et al.*, *Nucl. Instrum. Meth. A*, **412**, 454 (1998).
- [19] C. Arnaboldi, G. Pessina, and E. Previtali, *IEEE Trans. Nucl. Sci.*, **50**, 979 (2003).
- [20] E. Andreotti, C. Brofferio, L. Foggetta, A. Giuliani, B. Margesin, *et al.*, *Nucl.Instrum.Meth.*, **A664**, 161 (2012).
- [21] S. Pirro, *Nucl. Instrum. Meth. A*, **559**, 672 (2006).
- [22] C. Arnaboldi, G. Pessina, and S. Pirro, *Nucl. Instrum. Meth. A*, **559**, 826 (2006).
- [23] C. Arnaboldi *et al.*, *Nucl. Instrum. Meth. A*, **520**, 578 (2004).
- [24] M. Carrettoni and M. Vignati, *JINST*, **6**, P08007 (2011), arXiv:1106.3902 [physics.ins-det].
- [25] S. Ohya, *Nuclear Data Sheets*, **111**, 1619 (2010), ISSN 0090-3752.
- [26] S. Ohya, *Nuclear Data Sheets*, **102**, 547 (2004).
- [27] D. Watt and R. Glover, *Philos. Mag.*, **7**, 105 (1962), ISSN 1478-6435.
- [28] D. Munstermann and K. Zuber, *J.Phys.G*, **G29**, B1 (2003), arXiv:nucl-ex/0204006 [nucl-ex].
- [29] A. Alessandrello *et al.*, *Phys. Rev. C*, **67**, 014323 (2003).
- [30] J. Allison *et al.*, *IEEE Trans. Nucl. Sci.*, **53**, 270 (2006), ISSN 0018-9499.
- [31] J. D. Lewin and P. F. Smith, *Astropart. Phys.*, **6**, 87 (1996).
- [32] A. Alessandrello *et al.*, *Phys.Lett.*, **B408**, 465 (1997).
- [33] R. Bernabei *et al.*, *Eur.Phys.J.*, **C56**, 333 (2008), arXiv:0804.2741 [astro-ph].
- [34] C. Aalseth *et al.*, *Phys.Rev.Lett.*, **107**, 141301 (2011), arXiv:1106.0650 [astro-ph.CO].
- [35] G. Angloher *et al.*, *Eur.Phys.J.*, **C72**, 1971 (2012), arXiv:1109.0702 [astro-ph.CO].